

Conductive composite of UHMWPE and CB as a dynamic contact analysis sensor

Andrew C. Clark^a, Sunita P. Ho^b, Martine LaBerge^{a,*}

^aDepartment of Bioengineering, 501 Rhodes Research Center, Clemson University, Clemson, SC 29634, USA

^bDivision of Biomaterials and Bioengineering, D 3212, Department of Preventive and Restorative Dental Sciences, University of California San Francisco, San Francisco, CA 94143-0758, USA

Received 27 March 2005; received in revised form 22 September 2005; accepted 9 October 2005

Available online 21 November 2005

Abstract

There has long been a need to experimentally measure the dynamic contact conditions of important engineering tribological systems, especially those with polymeric bearing surfaces that prove difficult to model. In order to experimentally quantify the dynamic contact conditions of geometrically complex polymeric bearing surfaces, a composite sensor material has been developed. In this study, qualitative morphological analysis of virgin ultrahigh molecular weight polyethylene (UHMWPE) and carbon black (CB) powders, as well as UHMWPE and CB powder mixtures of varying percentages was performed using field emission scanning electron microscopy (FESEM). Quantitative structure and friction analysis using atomic force microscopy (AFM) was performed on cryoultrasectioned block surfaces of compression-molded CB/UHMWPE composite. In addition, the mechanical properties of the composites were quantified using tensile testing, and the force dependence of the electrical properties was examined under dynamic compressive loading.

The AFM results illustrated 5 μm wide CB-containing channels enclosing 150 μm diameter areas of UHMWPE within the CB/UHMWPE compression molded composite. Additionally, the dynamic coefficient of friction (μ) of UHMWPE-dominant regions was 0.18, similar to that reported in the literature (0.2). A Student's *t*-test with 95% confidence level indicated no significant difference ($p > 0.05$) between the elastic modulus of 8 wt% CB/UHMWPE composite (208.9 ± 11.1 MPa) and that of virgin UHMWPE control specimens (214.8 ± 21.1 MPa) processed under the same experimental conditions. Measurement of the force-dependent nature of the electrical resistance of different CB wt% composites showed that the resistances decreased nearly two orders of magnitude when the compressive loads were increased from 0 to 5 kN. The structure, friction, mechanical, and electrical property results of this study collectively showed that a partially conductive, segregated network composite of nanometer size CB in UHMWPE was obtained without high-shear mixing, that has electrical properties allowing the material to be used as a dynamic contact sensor.

© 2005 Elsevier Ltd. All rights reserved.

Keywords: Ultra-high molecular weight polyethylene (UHMWPE); Contact pressure sensor; Segregated network polymer composite; Polymer bearing

1. Introduction

Wear particles from ultra high molecular weight polyethylene (UHMWPE) bearing surfaces of total joint replacement (TJR) prostheses have been shown to cause adverse biological reactions which can lead to loosening of the prosthesis, and ultimately to failure [1]. In order to reduce the wear generated in TJR prostheses, contributing factors, such as component geometry, loading conditions,

and the resulting contact stresses, must first be understood [1–3].

Many experimental methods have been used to measure both the contact stress and the contact area of the TJR prostheses including Fuji pressure-sensitive film [4–8], stereophotogrammetry [5], dye injection methods [9], silicon casting methods [10], piezoelectric transducers [11], micro-indentation transducers [12], and commercial electronic pressure transducers [6]. In comparison, the use of Fuji pressure sensitive film has been more successful than others. However, the stiffness of the film, overestimation and irreproducibility of contact stresses under dynamic

*Corresponding author. Tel.: +1 864 656 5557; fax: +1 864 656 4466.

E-mail address: laberge@clemson.edu (M. LaBerge).

conditions limits its use under dynamic conditions [5,8]. Other electronic transducer methods provide dynamic measurements with a spatial resolution. However, these methods introduce a different material of at least 75–100 μm thickness in between the articulating components, which could alter the contact conditions of TJR prostheses.

Carbon black (CB) is an economical, conductive filler that can be added to UHMWPE to create a conductive composite material [15–18]. Additionally, a composite that is partially conductive under no strain will become more conductive if it is placed under compressive strain [13,14]. Because most TJR prostheses utilize UHMWPE as a load-bearing material, making a sensor out of a conductive UHMWPE composite would be advantageous.

It has been shown that the main method of conduction in a CB-filled polymer is electron tunneling from one conductive particle to the next, known as “percolation”. Percolation requires inter-conductive particle distances to be 10 nm or less within a polymer [13]. As conductive particles are added to a composite such that the inter-particle distance is less than or equal to 10 nm, a small increase in the amount of conductive filler will cause a sharp increase in composite conductivity. This point is known as the “percolation threshold” [13].

The terminology used to describe CB is also important to distinguish. A *primary particle* of CB is the “particle size” as listed by the manufacturer and is generally a spherical nano-sized particle. However, the smallest “base unit” of CB that can be obtained in a dispersion is called an *aggregate*. Aggregates are generally considered indivisible and are made up of many CB primary particles. The typical size of a CB aggregate is usually 50–500 nm in size and varies according to the manufacturer of the CB. While aggregates are the *smallest* unit of CB that can be obtained in a CB-filled polymer, CB is most often found in *agglomerates*. Agglomerates are dense configurations of many aggregates held together by van der Waals forces [19]. The best possible dispersions of CB are those consisting of small CB aggregates with no large agglomerates. Therefore, the method of mixing CB with the polymer must apply enough energy to overcome the van der Waals forces that hold together the CB agglomerates.

Because UHMWPE has such a high melt viscosity, it is difficult to disperse CB using traditional methods. However, there are three main ways that CB can be dispersed in UHMWPE, including the solvent solution method [16,17], the sintering method [15], and the multi-polymer blend method [18,20]. The polymer-blend method is less desirable for engineering applications because superior mechanical and wear properties of UHMWPE are reduced due to the presence of another polymer [16]. Considerable research has been focused on using solvent solution methods to dissolve the UHMWPE followed by mixing in CB [16,17]. However, the solvent solution method requires large percentages of CB to obtain conductivity, which could lead to inferior mechanical properties of

the resulting composite [21]. The sintering method is a form of compression molding, a method used to convert UHMWPE powder into a solid form [22].

In comparison to other ways of processing a CB/UHMWPE composite, sintered UHMWPE composites require less conductive filler because they form a segregated network [15,23]. Segregated network conductive composites have an internal morphology defined by small volumes of polymer that contain the conductive filler surrounded by larger volumes of polymer that contain no conductive filler.

This study focuses on the morphology, mechanical, and electrical properties of a composite sensor material of UHMWPE and CB that can measure dynamic contact stresses resulting from mechanical loading [24]. In order to prepare such a material, the following objectives were defined: (1) investigate the morphology of virgin UHMWPE and CB powders and UHMWPE and CB powder mixtures using field emission scanning electron microscopy (FESEM); (2) investigate the segregated-network structure of a processed CB/UHMWPE composite using atomic force microscopy (AFM); (3) perform a comparison study between the elastic modulus of compression-molded CB/UHMWPE composite and compression-molded virgin UHMWPE; and (4) provide an insight into the mechanisms of the force-dependent nature of the composite’s electrical resistance; the desired property that should allow the CB/UHMWPE composite material to serve as a dynamic contact stress sensor.

2. Materials and methods

2.1. Mixing of UHMWPE and CB powders and specimen preparation for FESEM and AFM

A common, medical-grade UHMWPE powder (GUR 1150, Ticona Engineering Polymers, Florence, KY), with an average particle size of 100 μm , and a conductive, furnace black CB (Printex L-6, Degussa Huls, Dusseldorf, Germany), with an average primary particle size of 18 nm, were used in this study. In order to mix the UHMWPE powder and the CB powder, predetermined amounts of each powder were placed in a 120 mL plastic specimen container and initially manually shaken for 5 min to obtain CB weight percentages of 0.25, 0.5, 1, and 8 wt%. The specimens were then mixed for 10 min on a laboratory vortex (Vortex Genie, Scientific Industries, Inc., Bohemia, NY) at the maximum speed setting.

Field emission scanning electron microscopy (FESEM-4700, Hitachi, Tokyo, Japan) was used to characterize the morphology of the composite cross-sections and the pre-processed powders using a 1 keV electron energy beam. All specimens viewed under FESEM were adhered to a 1.5 cm diameter aluminum disk using double-sided adhesive carbon tape. The powders examined under FESEM were virgin CB, virgin UHMWPE, 1 wt% CB/UHMWPE, and 8 wt% CB/UHMWPE. The compression-molded

composite of 8 wt% CB/UHMWPE was cryoultrasectioned at -150°C (glass transition temperature— T_g of UHMWPE is -120°C) [25] using a diamond knife (Micro Star Technologies, Huntsville, TX) and a CR-X cryoultramicrotome (Ventana Microscopy Products, Tucson, AZ). The morphology of the cryoultrasectioned block surface was first characterized using an AFM followed by FESEM using 1 keV electron energy beam.

2.2. Compression molding and specimen preparation for light microscopy

Both virgin UHMWPE powder and the four CB/UHMWPE powder mixtures (0.25, 0.5, 1, and 8 wt% by weight) were compression-molded into, rectangular sheets 12 cm long, 8.5 cm wide, and 2 mm thick using a mold consisting of a 2 mm thick Teflon frame sandwiched between 2 stainless-steel plates that were coated with Teflon mold release spray. The powders were processed in a laboratory press (Model C Laboratory Press, Fred S. Carver Inc., Wabash, IN) equipped with electric heaters for 20 min at a temperature of 205°C and a pressure of 10 MPa. The specimens were then quenched under pressure at a cooling rate of $50^{\circ}\text{C}/\text{min}$. Cryosectioning at -25°C with a steel blade (Microm Cryostat, Richard Allen Scientific, Kalamazoo, MI) was performed to produce $30\mu\text{m}$ thick cross-sections that were placed on glass slides and viewed at various magnifications between $40\times$ and $1000\times$ (Diaphot 300 Inverted Microscope, Nikon, Melville, NY).

2.3. AFM on ultrasectioned CB/UHMWPE composites

Cryoultrasectioned blocks of compression-molded 8 wt% CB/UHMWPE composites were mounted on 1.5 cm diameter steel disks using double sided adhesive tape. The specimens were analyzed using a contact mode atomic force microscope (Nanoscope E, DI-Veeco Instruments Inc., Santa Barbara, CA). Both topography and friction coefficients were qualitatively and quantitatively analyzed. The surfaces of the specimens were scanned at a frequency of 2 Hz using a commercially available silicon nitride (Si_3N_4) square pyramidal tip attached to a calibrated 'V' shaped cantilever with a normal spring constant equal to $0.025 \pm 0.004 \text{ N/m}$ [26]. Lateral force microscopy was used to evaluate the dynamic friction coefficient (μ) [26] of ultrasectioned-compression-molded composites under ambient conditions on six different areas.

2.4. Tensile testing of compression-molded CB/UHMWPE composites

In order to obtain comparative material properties of the composites, tensile testing was performed. Specimens with a gage length of 20 mm, a width of 4.9 mm, and a thickness of 2 mm were cut from the compression-molded sheets with a die following ASTM standards [27]. A servo-hydraulic testing system with a 10 kN load cell (Instron 8874, Instron

Corporation, Canton, MA) was used to perform tensile tests. Four specimens of each composite (and the control) were tested to failure at a constant strain rate of 5 mm/s. The resulting stress-strain curves were used to determine the elastic modulus, the ultimate strength, the yield strength, and the percent elongation at break. Student's *t*-tests with confidence levels of 95% were performed to determine significant differences in the elastic modulus values between the control specimens and the CB/UHMWPE composites.

2.5. Load vs. resistance response of UHMWPE/CB composites

The electrical resistances of the composites were measured as a function of compressive load using a servo-hydraulic testing system (Instron 8874, Instron Corporation, Canton, MA). In order to perform these tests, a voltage divider circuit was used, where the voltage drop across a reference resistor was measured with a data acquisition system (NuDaq PCI 9812, Adlink Technology Inc., Chungo City, Taiwan), and the resistance of the CB/UHMWPE composite was calculated using Ohm's law. Plots of resistance as a function of applied load were prepared for the 0.5, 1, and 8 wt% CB composites.

A servo-hydraulic testing system (Instron 8874, Instron Corporation, Canton, MA) was used to determine the electrical response of the composite under cyclic compressive loads. The data acquisition system was used to measure the voltages corresponding to resistance and load.

3. Results

3.1. Morphology of virgin UHMWPE and CB powders, and CB/UHMWPE powder mixtures using field emission scanning electron microscopy (FESEM)

FESEM examination of virgin CB powder showed $10\mu\text{m}$ diameter CB agglomerates (Fig. 1a) with loosely attached CB aggregates (Fig. 1b) formed by 50 nm diameter CB primary particles (circled section of Fig. 1b).

A FESEM micrograph of a UHMWPE powder particle is shown in Fig. 2. The surface of the particle has a rough texture and the size ranged from 50 to $200\mu\text{m}$ (Fig. 2a). Higher magnification shows that the particle is made up of many sub-micron spheroids held together by nanometer fibrils surrounded by varying amounts of free space (Fig. 2b). Fig. 2b shows voids and occlusions on the UHMWPE particle surface that are bigger than CB agglomerates (Fig. 1b). Based on Figs. 1 and 2 can be noticed that a CB aggregate is 3 orders of magnitude smaller than an UHMWPE particle.

Fig. 3 shows FESEM micrographs of the 1 wt% CB/UHMWPE powder mixture. Higher magnification of the composite powder shows UHMWPE spheroids and fibrils with CB aggregates enmeshed within the spheroid and fibril network (Fig. 3b).

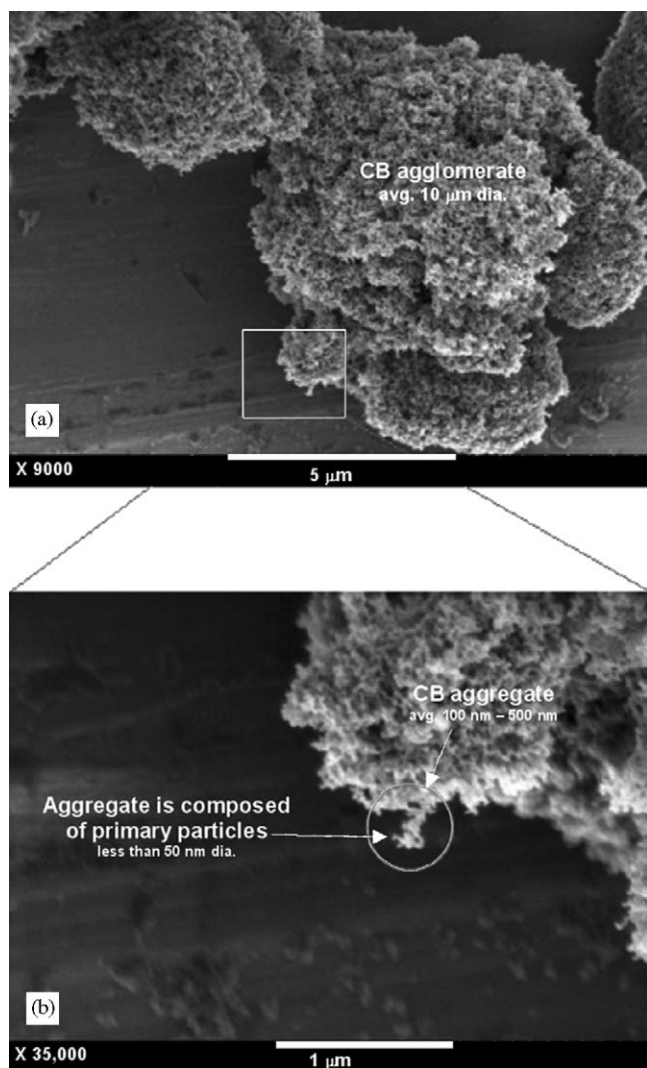


Fig. 1. FESEM (1 keV) images of virgin CB powder.

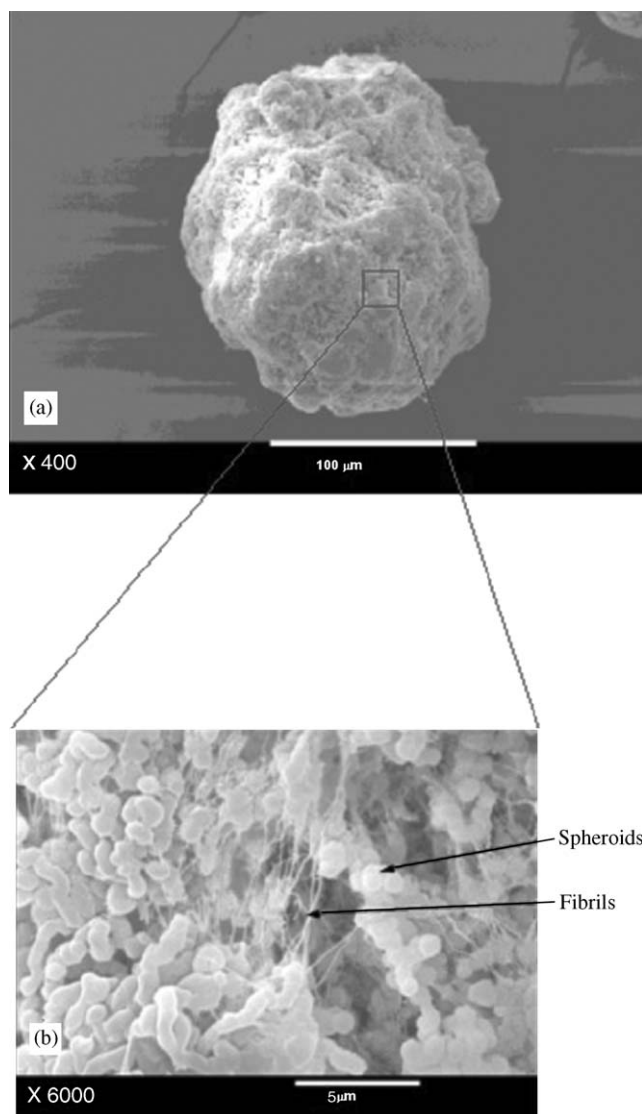


Fig. 2. FESEM (1 keV) images of virgin UHMWPE powder showing a particle of 150 μm diameter (a) and higher magnification of the particle surface (b).

Fig. 4 shows FESEM micrographs of the 8% CB/UHMWPE powder mixture. Higher magnification (Fig. 4b) of the composite powder shows a surface texture similar to that of pure CB as seen in Fig. 2. Based on the 3 orders of magnitude difference between a CB aggregate and UHMWPE particle, it was possible to obtain a uniform coating of CB aggregates on UHMWPE particles.

3.2. Morphology and friction coefficients of CB/UHMWPE compression-molded composite with field emission scanning electron microscopy and AFM

A representative cross-section of the 8wt% CB/UHMWPE compression-molded composite is shown in a light micrograph (Fig. 5a) and higher magnification FESEM micrographs (Figs. 5b and c). The boundary of a channel region is shown in Fig. 5b. Fig. 5c shows very high magnification of the channel region where small CB

aggregates and primary particles appear to be well dispersed in the UHMWPE.

Fig. 6 shows AFM scans of the cryoultrasected surface of the 8 wt% CB/UHMWPE composite. Frictional force microscopy identified distinct regions of higher and lower μ . The μ in a channel region was 0.11 ± 0.03 and μ in a non-channel region was 0.18 ± 0.04 . The morphology of the AFM micrograph (Fig. 6a) is similar to the light microscopy micrograph (Fig. 5a). Both low (light microscopy—Fig. 5a) and high (AFM—Fig. 6a) magnifications reveal CB channels within the CB/UHMWPE compression-molded composite.

3.3. Mechanical properties of compression-molded UHMWPE control and CB/UHMWPE composites

Representative stress–strain curves for the CB/UHMWPE composites and UHMWPE control are shown

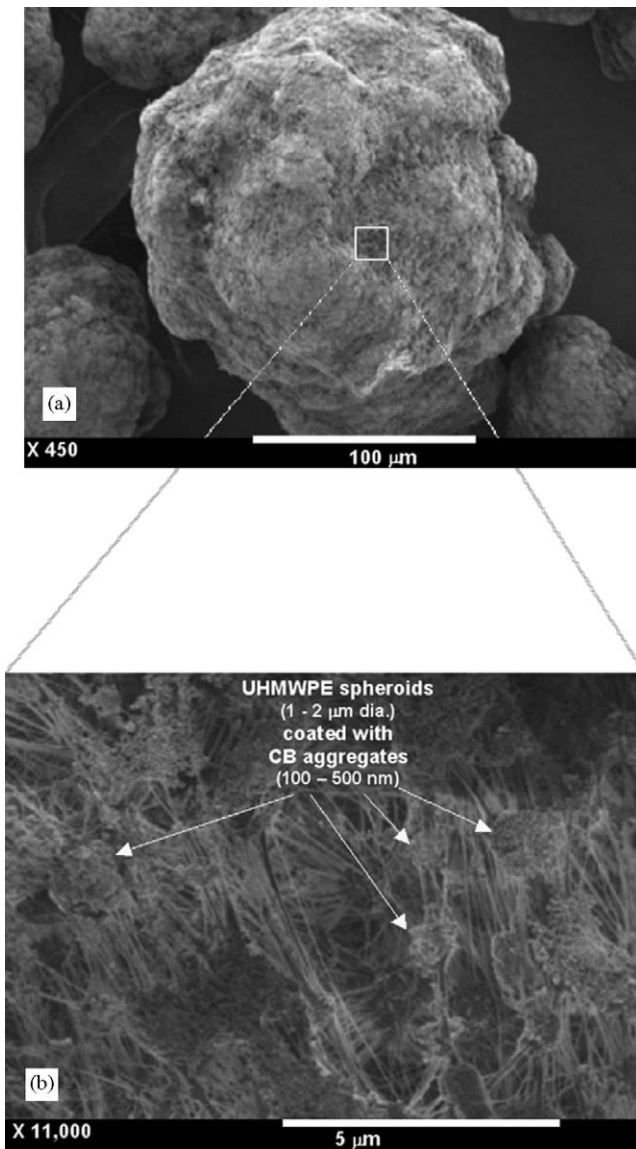


Fig. 3. FESEM (1 keV) of 1 wt% CB/UHMWPE powder.

in Fig. 7. The mechanical properties obtained from the tensile tests can be seen in Table 1. Student's *t*-tests with confidence levels of 95% indicated no significant differences ($p > 0.05$) between the elastic modulus values of the 0.25, 0.5, 1, and 8 wt% CB/UHMWPE composites and the virgin UHMWPE control specimens.

3.4. Electrical response of CB/UHMWPE composites

Fig. 8 shows a plot of the resistance as a function of the compressive load applied to the CB/UHMWPE composites of 0.5, 1, and 8 wt%. The slope of each line is similar, with the value of resistance changing by two orders of magnitude for each composite. Additionally, the *y*-intercepts of each line are different, indicating that the 0.5 wt% composite has the highest values of resistance and the 8 wt% composite has the lowest values of resistance. The

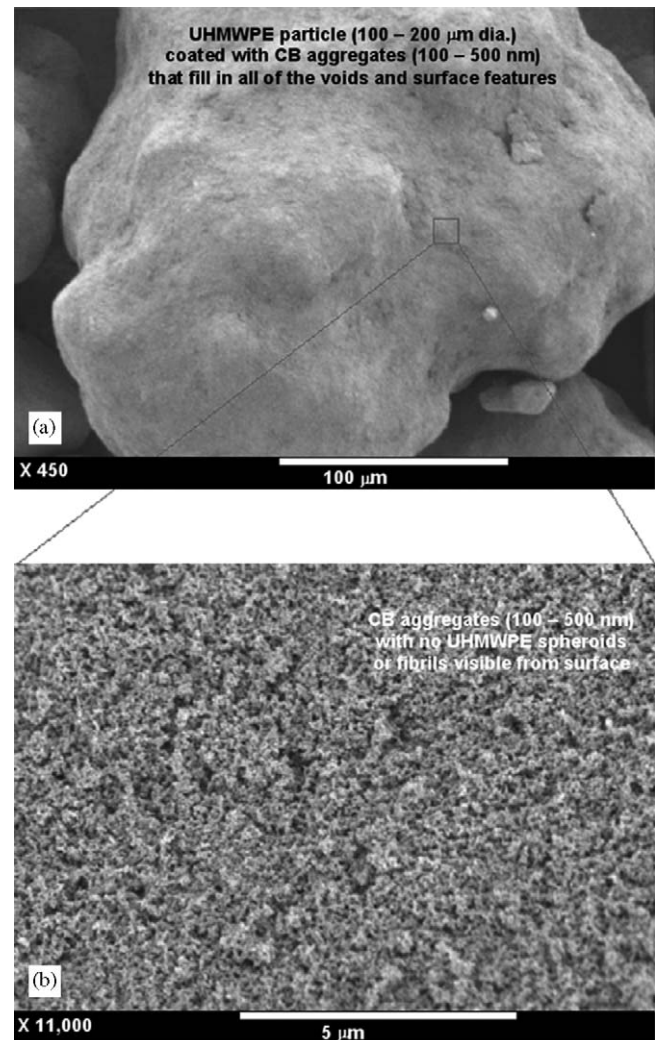


Fig. 4. FESEM (1 keV) of 8 wt% CB/UHMWPE powder mixture.

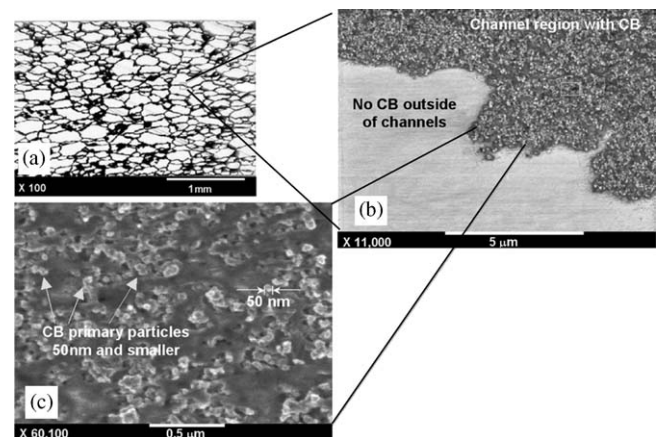


Fig. 5. Cryoultrasectioned (-150°C) 8 wt% CB/UHMWPE compression-molded composite showing segregated network structure with light microscopy (a), and higher magnification of the channel region with FESEM (1 keV) (b and c).

high regression coefficients indicate a good correlation between applied load and the resulting resistance of the respective composite materials.

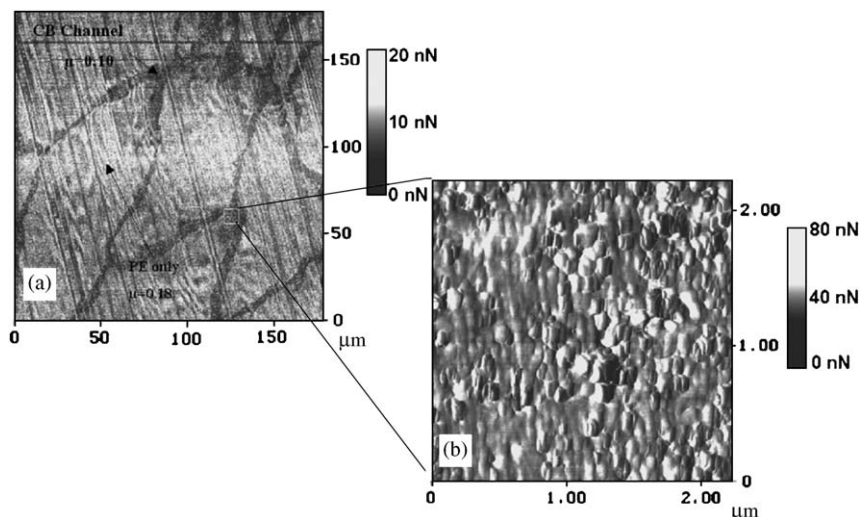


Fig. 6. AFM frictional force plots of cryoultrasectioned (-150°C) 8 wt% CB/UHMWPE compression-molded composite showing channel and non-channel regions (a), and higher magnification of a channel region (b).

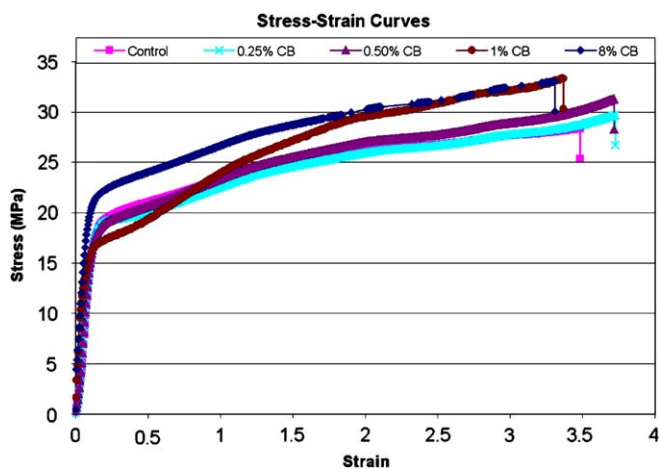


Fig. 7. Representative stress-strain curves.

When the values of resistance are normalized (Fig. 9) it becomes clear that the slope of each line is similar, suggesting that the amount of CB only affects the magnitude of the resistances measured. Thus, the relative response to applied load appears to be independent of the amount of CB. It should be mentioned that the control specimen and the 0.25 wt% CB specimen had high resistance for all loads tested and are not shown on the graphs.

Fig. 10 shows the raw voltage values corresponding to the compressive load, the compressive displacement, and the resistance of the 8 wt% CB/UHMWPE while the composite was loaded cyclically with a Haversine wave at 1 Hz. The top curve corresponds to the compressive stress, the middle curve corresponds to the compressive strain, and the bottom curve corresponds to the resistance of the sensor material.

4. Discussion

In this study, the use of FESEM allowed characterization of the materials without carbon or gold coating by using a low-energy electron beam of 1 keV. The coating necessary with the traditional scanning electron microscopy (SEM) technique would have obscured the nanometer voids and micrometer structural features in the UHMWPE particle. Additionally, the higher energy electron beam used with traditional SEM would cause the nanometer fibrils and micrometer spheroids to melt making the UHMWPE particles falsely appear smoother (data not reported, but observed when using a traditional SEM).

It is also important to note that the CB/UHMWPE composite cross-sections were obtained through cryoultramicrotomy at -150°C . This involved sectioning the UHMWPE composite at a temperature well below the T_g (-120°C) to eliminate the possibility of the blade causing plastic flow of the polymer, which would have possibly concealed any CB particles within or below the sectioned surface [25].

Because the diameter of a CB aggregate is 3 orders of magnitude smaller than the diameter of a UHMWPE particle, the CB aggregates coat the surface of the UHMWPE particles uniformly (Fig. 4). The thickness of the coating increases as the amount of CB in the CB/UHMWPE powder mixture increases.

In general, polymer powders build up electrostatic charges when stored in non-conductive plastic containers [23,28]. In this study, the UHMWPE powder was stored in a plastic container allowing it to develop electrostatic charges on the surfaces of the particles. Addition of CB powder to the UHMWPE powder in a non-conductive, plastic container could have caused the neutrally charged agglomerates to be attracted to the charged UHMWPE particles, resulting in a uniform coating.

Table 1

Average ($n = 4$) mechanical properties determined from tensile tests

$n = 4$	Control	0.25%	0.50%	1%	8%
Young's modulus (MPa)	214.8 ± 21.1	208.4 ± 7.68	211.9 ± 7.74	212.6 ± 6.82	208.9 ± 11.1
Tensile strength (MPa)	30.8 ± 3.98	29.1 ± 2.23	32.6 ± 3.49	31.9 ± 2.43	31.7 ± 1.03
Yield strength (MPa)	17.8 ± 0.75	18.0 ± 0.87	17.8 ± 0.93	15.2 ± 0.96	22.2 ± 1.07
Elongation at break (%)	390 ± 77.0	360 ± 18.0	390 ± 18.0	340 ± 23.0	290 ± 41.0

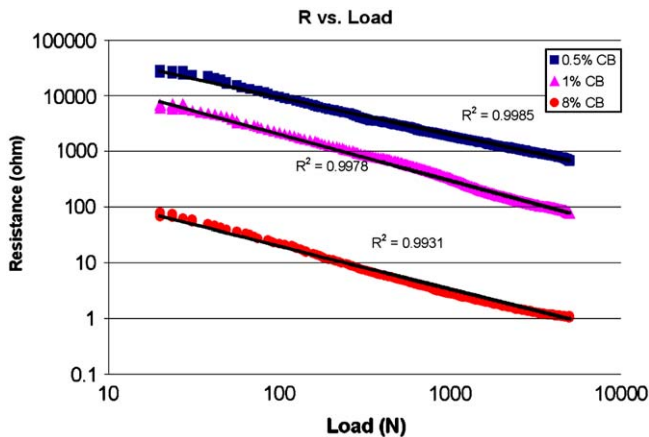


Fig. 8. Resistance vs. load in log scale for 0.5, 1, and 8 wt% CB/UHMWPE composites.

The FESEM and the frictional force microscopy micrographs show that individual CB aggregates and primary particles are well dispersed within the channel region of the composite (Figs. 5 and 6). This can be determined from the scale on respective figures, which illustrate the size of the CB primary particles and small aggregates in the composite to be under 200 nm, with some less than 50 nm. This agrees with the CB primary particle size of 18 nm as reported by the manufacturer.

Additionally, Fig. 5c illustrates the distances between many of the individual CB primary particles and aggregates are very small, perhaps nearing the inter-particle distance of 10 nm necessary for optimum electrical conductivity of the composite. Many such conductive paths where the CB primary particles and aggregates are spaced by no more than 10 nm can be traced within the micrographs.

The images in Fig. 5 of the compression-molded composite show that the interface of the CB/UHMWPE channel region with the UHMWPE-only region is abrupt, showing that the CB particles were not able to flow while the UHMWPE was above its melt temperature due to its high melt viscosity during the compression molding process. Knowing that this is a cross-section of the composite, it can be visualized that when the CB-coated UHMWPE particles were compression molded above the melt temperature of UHMWPE ($T_m = 130^\circ\text{C}$), the particles fused together, confining the CB to a three-dimensional channel network within the composite. Similar findings have been reported in the literature for composites

of nano-sized conductive fillers mixed with larger polymer and ceramic substrate particles [21,29]. This special type of conductive composite is referred to as a *segregated network* material since the conductive portions of the composite are contained in a channel-like network within the composite.

The set of images in Fig. 5 illustrates how the composite is able to have such a low percolation threshold compared to CB/UHMWPE mixtures prepared using other methods, such as solution mixing [16,17]. This set of images also provides insight into why the addition of CB at these small amounts (up to 8 wt% by weight) might be expected to have little effect on the mechanical properties of bulk UHMWPE. Because of the segregated network structure, the majority of the volume of the bulk CB/UHMWPE composite material is occupied by virgin UHMWPE. The actual volume occupied by the conductive UHMWPE-CB composite (optically black area in Fig. 5a) is only a fraction of the total volume of the bulk specimen.

The AFM images at higher magnification (Fig. 6) confirm that the channel region (seen in Fig. 5c) shows both CB and UHMWPE. The high magnification AFM (Fig. 6b) and FESEM (Fig. 5c) images are approximately the same scale (2 μm across the bottom edge). The AFM micrographs contain distinct regions of CB-dominant (harder; $\mu = 0.11$) and UHMWPE-dominant (softer; $\mu = 0.18$) material. The AFM data suggest that: (1) the morphology was similar to that observed using FESEM; (2) the compression molding technique provides a composite material with a segregated-network type of structure; (3) an even dispersion of CB aggregates and primary particles necessary for effective conductance was obtained within the channel regions; and (4) the coefficient of friction (μ) of UHMWPE-dominant regions (0.18) within the CB/UHMWPE composite is similar to that reported in the literature (0.2) [26,32].

The elastic modulus values obtained from tensile testing were comparable to those obtained by Parasnis and colleagues [30] for thin-film UHMWPE specimens. The values obtained for tensile strength, yield strength, and elongation at break compare closely to the values cited in the literature [31]. Because the processing parameters of temperature, pressure, and time can greatly affect the mechanical properties of UHMWPE, the actual values obtained for the mechanical properties could be changed by modifying the processing conditions [29,30]. More importantly, the fact that the control specimens were compression molded using the same processing conditions as the composites allowed for a direct comparison between

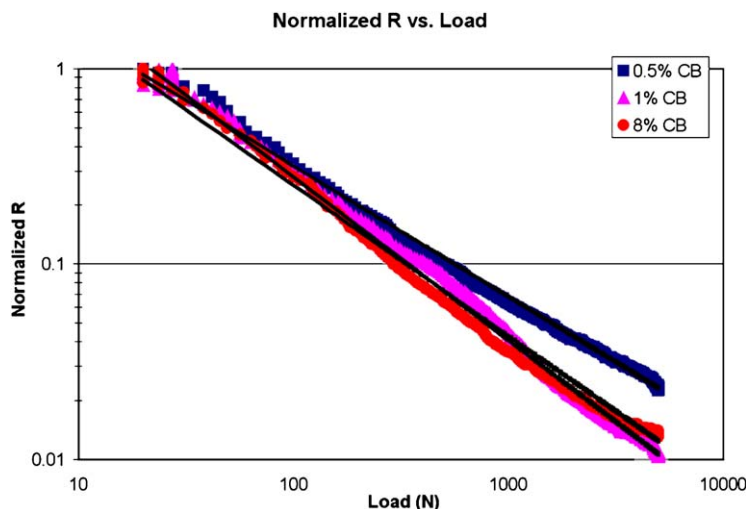


Fig. 9. Normalized resistance vs. load in log scale for 0.5, 1, and 8 wt% CB/UHMWPE composites.

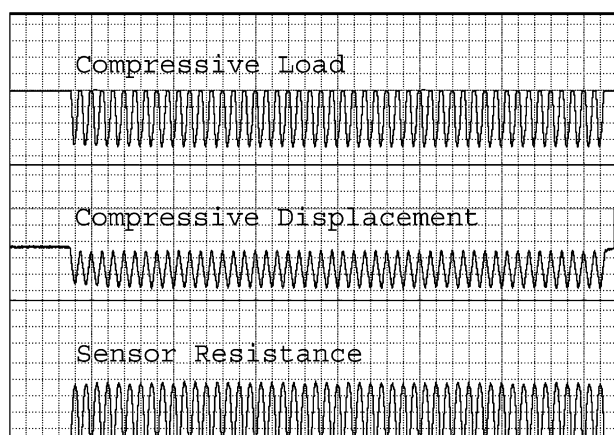


Fig. 10. Raw data from 1 Hz cyclic test of 1 wt% CB/UHMWPE composite.

specimens with and without CB. Thus, the mechanical properties were compared as a function of CB percentage, rather than as a function of processing conditions.

Monitoring the electrical resistance of the composite material while applying a compressive load revealed the force-dependent nature of the electrical properties of the material. Because of the nano-scale dispersion of the conductive filler, the electrical response of the material to applied load was nearly ideal for all of the composites tested. That is, the log of the resistance varied linearly with respect to the log of the applied load. This linear relationship makes the material well suited for use as a sensor. The data shows that the linear relationship holds true for 0.5, 1, and 8 wt%, with the difference between the three being the magnitude of the resistance. Because all three percentages show good sensor properties, the specific formulation could be chosen based on other criteria, such as the specifics of the measurement electronics.

The time-dependant response of the electrical properties is qualitatively illustrated in Fig. 10. The results of this

cyclic testing show that the peak voltage values corresponding to resistance remain nearly constant over many cycles, suggesting that some of the time-dependant properties such as viscoelasticity and stress relaxation do not influence the sensor output from the material during short-term cyclic loading patterns. Therefore, the data seem to indicate that the sensor material should be well suited for cyclic measurements since the readings do not degrade over time.

5. Conclusions

The nano-scale dispersion of CB within the channel regions of the CB/UHMWPE composites was obtained without conventional high-shear mixing methods. Because CB aggregates are approximately 1000 times smaller than UHMWPE particles, the compression-molded powder mixture formed a segregated-network type of conductive composite in which very low amounts of CB conductive filler were used to achieve the desired electrical properties for the sensor composite material. Because such low percentages of CB were able to be used for the sensor material, the mechanical properties of the composites tested were not significantly different from those of the virgin UHMWPE control specimens.

Acknowledgments

The authors would like to acknowledge Linda Jenkins of Clemson University, Clemson, SC, for her assistance in preparing slides for optical microscopy and John DesJardins of Clemson University for his assistance in mechanical testing of the specimens. The authors would also like to thank Michelin Americas Research and Development Corporation, Greenville, SC, for the use of the cryoultramicrotome and Dr. Joan Hudson of Clemson University for her assistance with electron microscopy.

References

- [1] Collier JP, Mayor MB, Surprenant VA, Surprenant HP, Dauphinais LA, Jensen RE. The biomechanical problems of polyethylene as a bearing surface. *Clin Orthop* 1990;261:107–13.
- [2] Collier JP, Mayor MB, McNamara JL, Surprenant VA, Jensen RE. Analysis of the failure of 122 polyethylene inserts from uncemented tibial knee components. *Clin Orthop* 1991;273:232–42.
- [3] Sathasivam S, Walker PS. Optimization of the bearing surface geometry of total knees. *J Biomech* 1994;27(3):255–64.
- [4] Postak PD, Heim CS, Greenwald AS. Tibial plateau surface stress in TKA: a factor influencing polymer damage—series IV—PCL substituting designs. *Orthop Trans* 1996;20(1):175.
- [5] Ateshian GA, Kwak SD, Soslowsky LJ, Mow VC. A stereophotogrammetric method for determining in situ contact areas in diarthrodial joints, and a comparison with other methods. *J Biomech* 1994;27(1):111–24.
- [6] Harris ML, Morberg P, Bruce WJM, Walsh WR. An improved method for measuring tibiofemoral contact areas in total knee arthroplasty: a comparison of K-scan sensor and Fuji film. *J Biomech* 1999;32:951–8.
- [7] Matsuda S, Whiteside LA, White SE. The effect of varus tilt on contact stresses in total knee arthroplasty: a biomechanical study. *Orthopedics* 1999;22(3):303–7.
- [8] Liao JJ, Hu CC, Cheng CK, Huang CH, Lo WH. The influence of inserting a Fuji pressure sensitive film between the tibiofemoral joint of knee prosthesis on actual contact characteristics. *Clin Biomech* 2001;16:160–6.
- [9] Black JD, Matejczyk MB, Greenwald AS. Reversible cartilage staining technique for defining articular weight-bearing surfaces. *Clin Orthop Relat Res* 1981;159:265–7.
- [10] Fukubayashi T, Kurosawa H. The contact area and pressure distribution pattern of the knee—a study of normal and osteoarthrotic knee joints. *Acta Orthop Scand* 1980;51:871–9.
- [11] Manouel M, Pearlman HS, Belakhlef A, Brown TD. A miniature piezoelectric polymer transducer for in-vitro measurement of the dynamic contact stress-distribution. *J Biomech* 1992;25(6):627–35.
- [12] Ahmed AM, Burke DL. In-Vitro measurement of static pressure distribution in synovial joints—Part I: tibial surface of the knee. *J Biomech Eng* 1983;105:216–25.
- [13] Sherman RD, Middleman LM, Jacobs SM. Electron transport process in conductor-filled polymers. *Polym Eng Sci* 1986;23(1):36–46.
- [14] Tang H, Chen X, Tang A, Luo Y. Studies on the electrical conductivity of carbon black filled polymers. *J Appl Polym Sci* 1996;59:383–7.
- [15] Chan CM, Cheng CL. Electrical properties of polymer composites prepared by sintering a mixture of carbon black and ultra-high molecular weight polyethylene powder. *Polym Eng Sci* 1997;37(7):1127–36.
- [16] Bin Y, Xu C, Agari Y, Matsuo M. Morphology and electrical conductivity of ultrahigh-molecular-weight polyethylene-low-molecular-weight polyethylene-carbon black composites prepared by gelation/crystallization from solutions. *Colloid Polym Sci* 1999;277:452–61.
- [17] Xu C, Bin Y, Agari Y, Matsuo M. Morphology and electric conductivity of cross-linked polyethylene-carbon black blends prepared by gelation/crystallization from solutions. *Colloid Polym Sci* 1998;276:669–79.
- [18] Breuer O, Tzur A, Narkis M, Siegmund A. HIPS/gamma-irradiated UHMWPE/carbon black blends: structuring and enhancement of mechanical properties. *J Appl Polym Sci* 1999;74:1731–44.
- [19] Accorsi JV. The impact of carbon black morphology and dispersion on the weatherability of polyethylene. Cabot Corporation. Presented at the international wire & cable symposium, Atlantic City, November 18, 1999.
- [20] Feng J, Chan CM. Double positive temperature coefficient effects of carbon black-filled polymer blends containing two semicrystalline polymers. *Polymer* 2000;41:4559–65.
- [21] Breuer O, Tchoudakov R, Narkis M. Electrical properties of structured HIPS/gamma-irradiated UHMWPE/carbon black blends. *Polym Eng Sci* 2000;40:1015–24.
- [22] Lewis G. Polyethylene wear in total hip and knee arthroplasties. *J Biomed Mater Res—Appl Biomater* 1997;38:55–75.
- [23] Bouchet J, Carrot C, Guillet J. Conductive composites of UHMWPE and ceramics based on the segregated network concept. *Polym Eng Sci* 2000;40(1):36–45.
- [24] Clark AC, LaBerge M, Clemson University assignee. Contact sensors and methods for making same. USPTO patent pending, February 15, 2005.
- [25] Ho SP, Riester L, Drews M, Boland T, LaBerge M. Effects of the sample preparation temperature on the nanostructure of compression moulded ultrahigh molecular weight polyethylene. *Proc Inst Mech Eng [H]* 2002;216(2):123–33.
- [26] Ho SP, Carpick RW, Boland T, LaBerge M. Nanotribology of Co–Cr–UHMWPE TJR prosthesis using atomic force microscopy. *Wear* 2002;253:1145–55.
- [27] ASTM D5937-96: determination of tensile properties of moulding and extrusion plastics. Annual Book of ASTM Standards, vol. 08.03, 1996.
- [28] Krishnamurthy V, Kamel IL. Cold compaction and sintering of ultrahigh-molecular-weight polyethylene containing a segregated iron network. *Polym Eng Sci* 1989;29(8):564–72.
- [29] Miller K, Ramani K. Process-induced residual stresses in compression molded UHMWPE. *Polym Eng Sci* 1999;39(1):110–8.
- [30] Parasnis C, Ramani K. Analysis of the effect of pressure on compression moulding of UHMWPE. *J Mater Sci: Mater Med* 1998;9:165–72.
- [31] Li S, Burstein AH. Current concepts review: ultra-high molecular weight polyethylene. *The J Bone J Surg* 1994;76-A(7):1080–90.
- [32] Huang P, Salinas-Rodriguez A, Lopez HF. Tribological behaviour of cast and wrought Co–Cr–Mo implant alloys. *Mater Sci Technol* 1999;15(11):1324–30.